HHS Public Access

Author manuscript

Biochim Biophys Acta. Author manuscript; available in PMC 2016 December 01.

Published in final edited form as:

Biochim Biophys Acta. 2015 December ; 1854(12): 1809–1815. doi:10.1016/j.bbapap.2015.09.001.

A Rationally Designed Mutant of Plasma Platelet-Activating Factor Acetylhydrolase Hydrolyzes the Organophosphorus Nerve Agent Soman*

Stephen D. Kirby[1,2], **Joseph Norris**[1], **Richard Sweeney**[1], **Brian J. Bahnson**[2], and **Douglas M. Cerasoli**[1]

[1]U.S. Army Medical Research Institute of Chemical Defense, APG, MD 21010, United States

[2]Department of Chemistry & Biochemistry, University of Delaware, Newark, Delaware 19716, United States

Abstract

Organophosphorus compounds (OPs) such as sarin and soman are some of the most toxic chemicals synthesized by man. They exert toxic effects by inactivating acetylcholinesterase (AChE) and bind secondary target protein. Organophosphorus compounds are hemi-substrates for enzymes of the serine hydrolase superfamily. Enzymes can be engineered by amino acid substitution into OP-hydrolyzing variants (bioscavengers) and used as therapeutics. Some enzymes associated with lipoproteins, such as human plasma platelet-activating factor acetylhydrolase (pPAF-AH), are also inhibited by OPs; these proteins have largely been ignored for engineering purposes because of complex interfacial kinetics and a lack of structural data. We have expressed active human pPAF-AH in bacteria and previously solved the crystal structure of this enzyme with OP adducts. Using these structures as a guide, we created histidine mutations near the active site of pPAF-AH (F322H, W298H, L153H) in an attempt to generate novel OP-hydrolase activity. Wild-type pPAF-AH, L153H, and F322H have essentially no hydrolytic activity against the nerve agents tested. In contrast, the W298H mutant displayed novel somanase

*This research was supported by the Defense Threat Reduction Agency – Joint Science and Technology Office, Medical S&T Division. Funding was also obtained from NIH grants 8P30GM103519 from the National Institute of General Medical Sciences, and 5R01HL084366 from the National Heart, Lung, and Blood Institute to B.J.B. The views expressed in this manuscript are those of the authors and do not reflect the official policy of the Department of Army, Department of Defense, or the U.S. Government.

To whom correspondence should be addressed: Stephen D. Kirby, Research Division, Physiology and Immunology Branch, U.S. Army Medical Research Institute of Chemical Defense, 3100 Ricketts Point Road, APG, MD 21010-5400, Tel.: (410) 436-2336; stephen.d.kirby.civ@mail.mil.

[3]The abbreviations used are: OP, organophosphorus compounds; AChE, acetylcholinesterase; pPAF-AH, plasma platelet-activating factor acetylhydrolase; BuChE, butyrylcholinesterase; CaE, carboxylesterase; WT, wild-type; Å, angstroms; PAF, platelet-activating factor; LDL, low density lipoprotein; HDL, high density lipoprotein; PDB, Protein Data Bank; VMD, Visual Molecular Dynamics program; M.O.E., Molecular Operating Environment program; EDTA, ethylenediaminetetraacetic acid; OD, optical density; A_{600}, absorbance at 600 nm; IPTG, isopropyl β-D-1-thiogalactopyranoside; DTT, dithiothreitol; PNPB, para-nitrophenyl butyrate; ε, extinction coefficient; v_0, initial velocity; K_M, Michaelis-Menten binding constant; V_{max}, maximum velocity; k_{cat}, turnover number; K_i, inhibition constant; DTNB, 5,5′-dithiobis-2-nitrobenzoic acid; GC/MS, gas chromatography/mass spectrometry; DFP, diisopropyl fluorophosphate; m/z, mass to charge ratio; k_{cat}/K_M, catalytic efficiency; *i*-face, interface binding surface; P_S, phosphorus (−) enantiomer; P_R, phosphorus (+) enantiomer; C_S, carbon (−) enantiomer; C_R, carbon (+) enantiomer; PON1, paraoxonase-1; GB, sarin; GD, soman; GA, tabun; GF, cyclosarin

activity with a k_{cat} of 5 min^{-1} and a K_M of 590 μM at pH 7.5. There was no selective preference for hydrolysis of any of the four soman stereoisomers.

Graphical abstract

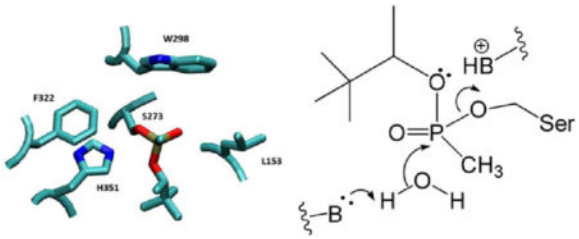

Keywords

nerve agents; organophosphorus compounds; plasma platelet-activating factor acetylhydrolase; bioscavenger; soman

1. INTRODUCTION

Anti-cholinesterase organophosphorus compounds (OPs) such as the chemical warfare nerve agents sarin and soman (Figure 1A), are among the most toxic substances synthesized by man, being highly lethal for mammals [1]. They pose a lethal threat to human life because they rapidly inhibit acetylcholinesterase (AChE), but they also inhibit other enzyme targets [2]. Current chemotherapeutic countermeasures against OP intoxication are effective, but can result in behavioral incapacitation and can have deleterious side effects if not given within a prescribed time frame after OP exposure or if their dosage is too high [1]. These unwanted side effects have necessitated the development of more efficacious alternative measures such as enzymes that neutralize or scavenge nerve agents (bioscavengers) and have little or no side effects [3]. Bioscavengers can bind and, in an ideal scenario, hydrolyze nerve agents in the plasma before they reach AChE targets in the peripheral and central nervous systems.

Organophosphorus compounds are potent inhibitors of enzymes of the serine hydrolase superfamily, which includes AChE, butyrylcholinesterase (BuChE), carboxylesterase (CaE) and plasma platelet-activating factor acetylhydrolase (pPAF-AH; EC 3.1.1.47). They act as hemi-substrates for these enzymes but become “locked” at the phosphorylation step as shown in Figure 1B. Typically, the dephosphorylation step is extremely slow because of unfavorable stereochemistry adopted around the adducted active site serine, which blocks the wild-type (WT) mechanism from hydrolyzing the adducted phosphoryl group. Thus, enzymes of the serine hydrolase superfamily have the potential to be reengineered through specific mutations into OP-hydrolyzing platforms that can be used as catalytic scavengers to afford protection against OP toxicity [4]. Starting from the structure of an inactivated serine hydrolase, site-directed mutations of amino acid residues surrounding the active site within 4–10 angstroms (Å) can influence interactions between the phosphorylated active site serine and an activated water molecule to enhance hydrolysis.

Historically, the enzymes found in the plasma that bind nerve agents (such as BuChE) were the first choice in providing an enzyme platform for engineering novel catalytic activity to degrade OPs. Limited success was met with the BuChE mutant G117H [5] and the double mutant G117H/E197Q to hydrolyze sarin, and later soman [6]. While the construction of these engineered bioscavengers with novel catalytic activity was encouraging, the pseudo first order rate constant of BuChE G117H for soman was found to be too slow to provide sufficient *in vivo* protection against this OP [5,7]. We sought other enzymes within the plasma that could serve as an enzyme platform for mutagenesis. Herein we describe engineering pPAF-AH with a general base catalyst in positions close to the active site serine, similar to those constructed in BuChE, in an attempt to improve dephosphorylation rates.

Plasma PAF-AH inactivates the potent phospholipid mediator platelet-activating factor (PAF) and other structurally similar bioactive lipids produced in response to oxidative damage [8]. PAF is an acetylated derivative of glycerophosphocholine with an ether linked 16-carbon chain attached to carbon 1, and it is poorly soluble in the aqueous phase. Produced by platelets, basophils, eosinophils, neutrophils, and endothelial cells, it modulates platelet aggregation, bronchoconstriction, inflammation, shock, and vascular ischemia leading to stroke [9]. Bound to both low-density lipoproteins (LDL) and high-density lipoproteins (HDL), pPAF-AH inactivates PAF by catalyzing a phospholipase A_2 esterolysis at the *sn*-2 position, producing lyso-PAF and acetate. Based on this activity and its association with lipoprotein in circulation, pPAF-AH is described as a lipoprotein-associated phospholipase A_2.

We have previously expressed and purified active human pPAF-AH in bacteria and solved the crystal structure with tabun (PDB 3F98), sarin (PDB 3F96) and soman (PDB 3F97) adducts [10]. Informed by these structures, we made a limited series of single point amino acid substitutions designed to explore novel dephosphorylation of the active site serine. We characterized the interactions of the pPAF-AH mutants with ester and OP substrates to determine their activity. Encouraging results from one mutation (W298H) show promise that a protein engineering approach with pPAF-AH can have utility in the development of biological scavengers capable of providing protection, *in vivo*, from these highly toxic OPs.

2. MATERIAL and METHODS

2.1 Molecular Modeling

Structures of human pPAF-AH [10] were used to identify residues of interest surrounding active site residues S273 and H351. While histidine mutations at positions W298, F322, and L153 are the focus of this project, other point mutations were constructed to explore how active site substitutions could influence substrate binding and catalysis. The following mutations were constructed: W298H, W298F, W298Y, W298D, W298A, F322H, F322R, F322K, and L153H. Modeling was conducted using the program VMD (Visual Molecular Dynamics, University of Illinois, Urbana-Champaign). We used the Site Finder application from the program M.O.E. (Molecular Operating Environment; Chemical Computing Group Inc., Montreal, Canada) to map the active site residues and void volume by packing 1 $Å^3$ spheres and applying solvation and void rules dictated by M.O.E. applications. Amino acid

alignment for pPAF-AH and other proteins was performed using the program ClustalW (Conway Institute, University College, Dublin, Ireland).

2.2 Bacterial Expression

Synthetic vector sequences of nine mutant pPAF-AHs and a WT pPAF-AH sequence were synthesized *de novo* (GeneArt AG, Germany) in the pGEX-4T3 vector (GE Healthcare, Mickleton, NJ) containing a glutathione-S-transferase fusion partner at the amino terminus and a linker region containing a thrombin cleavage site. Ten micrograms of the lyophilized plasmids were resuspended in tris-ethylenediaminetetraacetic acid (EDTA) buffer. One liter of Luria-Bertani Broth media plus ampicillin (50 μg/ml) was inoculated with BL21 DE3 cells (Invitrogen Life Technologies, Carlsbad, CA), after heat-shock transformation with 20 ng of expression vector containing the pPAF-AH synthetic vector. The cultures were grown at 37 °C until they reached 0.6 OD units at A_{600}. Cells were induced to express using 0.5 mM isopropyl β-D-1-thiogalactopyranoside (IPTG; Invitrogen Life Technologies, Carlsbad, CA) and harvested after 4 h of induction at 37 °C. Mock transformation and expression with empty pUC19 vector was processed in the same fashion as WT pPAF-AH.

2.3 Human pPAF-AH Purification

Bacterial cells were lysed by sonication on ice in lysis buffer (50 mM Tris, 150 mM NaCl, 1 mM EDTA, 0.5 mM dithiothreitol (DTT), 0.2% Triton DF-116, 1 mM phenylmethylsulfonyl fluoride at pH 8.0). Cellular debris was separated by centrifugation. Supernatant from the disrupted cell mixture was added to glutathione sepharose 4B resin (GE Healthcare, Mickleton, NJ) for 30 min at 4 °C with gentle inversion. The resin was washed 5 times with 4 bed volumes (40 ml) of wash buffer (50 mM Tris, 150 mM NaCl, 1 mM EDTA, 0.5 mM DTT, 0.2% Triton DF-116 at pH 8.0). The elution buffer was made from the wash buffer by the addition of 20 mM reduced glutathione. The column was eluted with 2 bed volumes (20 ml), and the elute was concentrated 30-fold using 10K molecular weight cut-off spin columns (EMD Millipore, Billerica, MA). Elution buffer was dialyzed against 10 mM Tris buffer pH 8.0. Protein concentrations were estimated using BCA™ protein assay kit (Thermo Fischer Scientific, Waltham, MA).

2.4 Substrate and Gas Chromatography/Mass Spectroscopy Assays

Assays for pPAF-AH activity were performed with either para-nitrophenyl butyrate (PNPB; Sigma–Aldrich, St. Louis, MO) or 2-thio PAF (Cayman Chemical Co., Ann Arbor, MI). PNPB was dissolved in ethanol and diluted to 5–1000 μM using 10 mM Tris buffer pH 8.0. Assays for PNPB hydrolysis were conducted by measuring the change in absorbance at 410 nm (extinction coefficient ε_{410} = 16,300 $M^{-1}cm^{-1}$ for nitrophenol) on a Spectramax Plus384 microplate reader (Molecular Devices Inc., Sunnyvale, CA). The K_M and V_{max} values were determined by fitting the data to the Michaelis-Menten equation ($v_0 = V_{max}[S]/(K_M + [S])$). Turnover number ($k_{cat}$) was determined by dividing V_{max} by total enzyme concentration. BuChE used in these assays was purified from outdated human plasma (Baxter BioScience).

The substrate 2-thio PAF was diluted to a stock concentration of 105 μM using 10 mM tris adjusted to various pH values. Assays were conducted as follows: 10 μL of 105 μM 2-thio PAF, and 5 μL of 20 mM 5,5′-dithiobis-2-nitrobenzoic acid (DTNB) were added to 190 μL

of 10 mM Tris in a modified Ellman assay [11]; 5 μL of protein sample was added to the mixture and read in a microplate reader at 412 nm for 1 h using the slope from the linear portion of the curve to determine rate. An extinction coefficient of 13,600 $M^{-1}cm^{-1}$ for the reaction product was used to convert A_{412} nm to concentration of consumed DTNB. Experiments were conducted at a single substrate concentration (5 μM), which was slightly above the critical micelle concentration for C-16 PAF at 1.1 μM [12].

The stereoselectivity of hydrolysis of soman by WT and mutant pPAF-AHs was studied using gas chromatography/mass spectrometry (GC/MS) methods modified from Yeung *et al.* [13]. All mutants were screened for OP hydrolase activity. Purified pPAF-AH was incubated at room temperature with a fixed concentration (1 mM) for screening specific activity or various concentrations of racemic soman (10.4 mM stock) to develop kinetic parameters. At various time points (t = 0, 15, 30, 45, and 60 mins), 100 μl of the mixture was extracted with an equal volume of dry ethyl acetate containing 50 μM diisopropyl fluorophosphates (DFP) as an internal standard. The majority of the organic layer containing the unreacted soman was removed and passed over type 4A (grade 514) alumina-silicate molecular sieve to remove water. Samples were transferred to 11 mm crimp top vials for GC/MS analysis. One-microliter samples were autoinjected and components separated using an Agilent 6890 gas chromatograph fitted with a 20 meter × 0.25 mm inside diameter Chiraldex gamma-cyclodextrin trifluoroacetyl column with 0.125 μm film thickness (Sigma–Aldrich). The gas chromatograph was interfaced to an Agilent 5973 mass spectrometer with an electronic impact ion source operated under selected ion monitoring mode. Three ions (m/z 69, 101 and 127) were monitored for DFP, and two ions (m/z 69 and 99) were monitored for soman. Quantification was accomplished using m/z = 127 for DFP and m/z 99 for soman. For each sample, the total area under the curve for each isomer was used to determine the relative stereoselectivity. Peaks were normalized against the internal standard DFP peak to account for pipetting and instrument sampling errors during sample analysis.

3. RESULTS

We have previously crystallized and refined OP adduct models of pPAF-AH (Figure 2A) following inactivation with tabun, sarin and soman [10]. Figure 2A depicts a ribbon structure of pPAF-AH adducted to soman [10]. From these structures we determined residues F322, W298, and L153 (Figure 2B) to be in close proximity to the active site serine (S273), which sits at the apex of a trough that provides potential binding sites for long, bulky substrates. These three residues of interest surround S273 and are essentially at the nine, twelve, and three o'clock positions, respectively, with the majority of the active site trough occupying the six o'clock position if S273 is consider the center point. W298 sits in a position at twelve o'clock and forms a "backboard" for the apex of the active site trough behind S273. In addition to these three sites, we mapped residues that define the active site pocket. Using the Site Finder application in M.O.E., residues identified as lining the active site of pPAF-AH and the percentage of each characteristic are listed in Table I. The volume of the active site void was calculated to be 828 $Å^3$. For comparison purposes, we also calculated the active site void for human BuChE (PDB 1P0I) to be 582 $Å^3$ using the same modeling software and parameters.

The effects mutations have on activity in pPAF-AH were examined against the ester substrates PNPB and 2-thio PAF. We were able to determine k_{cat} and K_M values from PNPB hydrolysis (Table II). PNPB esterolysis activity for mutants W298Y, W298D, W298A and L153H was not sufficient to develop kinetic parameters, because of either low activity or high variability among the data points. Mutations at the F322 position, which were all polar basic substitutions, displayed (on average) a 70% decrease in catalytic efficiency (k_{cat}/K_M). Only the mutations W298H and W298F displayed k_{cat}/K_M values that were 60% and 55% of WT, respectively. Surprisingly, K_M values were reduced for both mutants but were not significantly different from WT. A pH profile in 10 mM Tris buffer was conducted with 2-thio PAF against all the pPAF-AH mutants and WT to determine optimal activity (Figure 3). With the exception of W298H, all mutants showed less specific activity than WT at all pH values tested (pH 3.10, 4.90, 6.50, 6.90, 7.95 & 8.95). Wild-type pPAF-AH reached maximal activity at pH 7.95 The pH rate profile for W298H mirrored WT except that activity was elevated across all pH values measured, and W298H reached maximal activity at slightly more acidic conditions (pH 6.9). Although W298H showed enhanced activity against 2-thio PAF (Figure 3), it had reduced catalytic efficiency against PNPB (Table II). L153H was the only mutant tested that was inactive against both PNPB and 2-thio PAF.

Our long-term goal of developing pPAF-AH as a catalytic bioscavenger for OP nerve agents required analysis of the interactions and reactivity between the enzyme and an OP. The reactivity of AChE and BuChE with OP nerve agents is extremely fast, and a bimolecular rate constant for inactivation can be difficult to capture. It was surprising to find that wild-type pPAF-AH had an unusually slow reactivity with racemic soman (Figure 4). At room temperature, various molar ratios of enzyme to nerve agent (1:10, 1:100, and 1:1,000) for pPAF-AH and BuChE were examined. In the continuous presence of nerve agent, pPAF-AH required nearly 100 times more nerve agent to develop an inhibition curve that resembled that of BuChE (comparing BuChE:soman 1:10 & pPAF-AH:soman 1:1000). Even with this difference in molar ratios, pPAF-AH required nearly triple the time to reach zero activity. These results were unexpected and would not be an optimal choice for developing a catalytic bioscavenger.

Racemic soman hydrolysis was initially measured using a modified GC/MS assay and a fixed concentration of soman. Racemic soman is a mixture of four separate isomers (P_SC_S / P_SC_R / P_RC_S / P_RC_R), and the stereoselective preference for hydrolysis could be followed on a chiral column (Figure 5). Histidine mutants F322H and L153H showed no enhanced hydrolysis of racemic soman above those rates observed for wild-type pPAF-AH. These two mutants and wild-type pPAF-AH have relative activities less than 4 nmoles/hr/μg protein each for racemic soman. In contrast, W298H has relative activity for racemic soman hydrolysis closer to 26 nmoles/hr/μg. There was no difference between F322H, L153H, and wildtype values. Each stereoisomer was hydrolyzed by W298H with roughly equivalent rates (within error) demonstrating that W298H displays no stereoselective preference for hydrolysis of soman.

Subsequent experiments examined saturation curves for the W298H soman hydrolytic activity at pH 7.5 and 8.0 (Figure 6). Steady state kinetic parameters of W298H at pH 8 (n = 5) were observed to be nearly linear with no saturation of the curve. A maximal k_{cat} of 29

min^{-1} was developed with a calculated K_M of 6.8 mM. However, this was an extrapolation beyond the limits of our assay, since soman concentrations greater than 2 mM could not be used in experiments due to safety related constraints. At pH 7.5 (n = 3), a k_{cat} of 5 min^{-1} was determined with a K_M of 593μM. This represents a catalytic efficiency of 8.4×10^3 M^{-1} min^{-1}.

4. DISCUSSION

Serine hydrolases have the potential to be converted into OP hydrolyzing platforms because of the inherent nature of the OP inhibitors to act as hemi-substrates and to be locked into the first half of the esterolysis mechanism. After stereo-inversion around the adducted phospho-center, the face of the developing intermediate is protected from reactive nucleophiles (e.g., activated water molecule) coordinated by the native amino acid residues within the active site during the second half of the reaction, and any ensuing hydrolysis of the intermediate is blocked, leaving the enzyme in an inactivated state (Figure 1B). Two competing reactions will ensue: hydrolysis of the phospho-serine adduct, which is extremely slow for most esterases, or a mono dealkylation of the phospho-serine adduct which generates an “aged” enzyme. “Aging” rates are dependent on the type of OP used for inhibition, and “aged” enzymes are completely refractory to spontaneous or oxime-assisted reactivation. Recently two enzymes have been shown to resist aging of branched OP complexes; the non-aged crystal structures of human CaE complexed to soman and tabun [14], and PAF-AH 1b (a group VIII-PLA_2) complexed with sarin and soman [15] have been reported making them more attractive platforms to develop as catalytic bioscavengers for OP nerve agents.

Conditions may vary across the serine hydrolase family of enzymes, but two factors need to be satisfied for hydrolysis of the phosphorylated serine to be executed: access to water molecules and an opportunely positioned general base to activate the water molecule for addition onto the appropriate face of the phospho-enzyme intermediate. It can be postulated that pPAF-AH H351 is the primary base (together with its dyad partner D296) in the active site and is suited for hydrolysis of an esterified active site serine, but sits in an unfavorable position for hydrolysis of a phosphorylated serine. Substitution of a residue close to the active site serine to a different amino acid that is able to function as a general base catalyst is the model that we employed here and is the one that historically has held the most promise for engineering novel OP hydrolase activity [6]. It can be postulated that access to the phospho-serine adduct by the attacking water molecule for the W298H mutant is less restricted or positioned more accurately (~126° away from H351 and ~7Å from S273; Figure 2D) than for the other mutants tested due to the novel turnover observed in this mutant.

Previously, modest success was achieved by Broomfield and Millard [5] converting BuChE into a platform that could hydrolyze sarin, VX and other OP compounds by substituting a histidine for a glycine (G117H) at a key active site position, which partially forms the putative oxyanion hole. However, the G117H mutant of BuChE could not hydrolyze soman. Following another round of rational protein engineering, synergy ensued and soman hydrolysis was achieved with the addition of the E197Q mutation to the G117H platform [6]. Broomfield reported a rate constant for dephosphorylation after soman inhibition for

G117H/E197Q to be 0.06 min^{-1}. Here we achieved soman hydrolysis that is two orders of magnitude faster with the single point mutation of W298H and a k_{cat} of 5 min^{-1}. This is a remarkable achievement for any engineered enzyme platform but especially so for pPAF-AH, given that wild-type inactivation using soman is exceptionally slow (Figure 4). This is the first instance since BuChE G117H that OP-hydrolase activity with reportable rates has been created on any enzyme platform from a single amino acid substitution.

By developing rational, active site mutations in pPAF-AH, we have not only engineered a significant OP hydrolase bioscavenger, but also learned more about the catalytic mechanism and functional properties of pPAF-AH. While a full description of the catalytic mechanism and substrate binding sites will certainly require further mutations and experiments, these studies elucidate some facets of the mechanism. It is not surprising that most of the mutants, including W298H and W298F, lost significant activity against the PNPB substrate (Table II). W298 appears to be vital for substrate interactions with S273, based on geometric observations and the fact that substituting W298 with alanine (W298A) dramatically reduced activity for both ester substrates (Table II & Figure 3). On this assumption, it is reasonable that conservative substitutions like W298F retained a larger portion of activity compared to other mutants. Values for K_M across all the mutations were not significantly different from wild-type (Table II). The W298H substitution is unusual in that a polar charged (positive at pH < 6.5) group did not eliminate activity but instead only reduced it slightly for PNPB, and enhanced it for 2-thio PAF (Figure 3).

The ability of pPAF-AH to interact with substrates from both the aqueous and the lipid interfacial surface makes it an interesting candidate for development as a catalytic bioscavenger, as this enzyme could target OP substrates that partition into lipid dense compartments *in vivo* and environments *ex vivo*. Testing WT pPAF-AH in a more native state, perhaps in the presence of purified liposomes or artificial lipid rafts, may result in a better understanding of the interaction between pPAF-AH and OP inhibitors like soman. There is evidence to suggest that pPAF-AH may have its activity modulated by lipid composition and may undergo interfacial activation upon binding to lipoproteins [16].

During inactivation of serine hydrolases by soman, the product of inhibition is a chiral phosphorylated serine at the active site. The chirality adopted is dependent upon which of the two phosphorus stereoisomers of soman that reacted during phosphorylation. One possibility is that the more toxic stereoisomers (P*s*C*s*/$_R$) of soman [17] bind more rapidly, forming a product that is more difficult to hydrolyze because of its configuration. Alternatively, adduct formation with the P*s* isomers may result in a configuration that is more susceptible to a subsequent dealkylation process (e.g., “aging”) that prevents enzyme reactivation. In these experiments we separated each soman stereoisomer after hydrolysis of the racemic compound to identify stereoselectivity, if any. Therefore we must consider differences observed in activities when comparing rates of hydrolysis for “racemic” OP compounds versus hydrolysis of pure enantiomers in solutions for future experiments. Preferential hydrolysis of the more toxic stereoisomers of OP nerve agents is a major consideration in engineering and development of a catalytic bioscavenger. As can be seen from the BuChE G117H/E197Q data [6], there are differences in the rates of hydrolysis for each stereoisomer of soman. We observed no significant difference in the rates of hydrolysis

for any of the soman stereoisomers when using W298H pPAF-AH as seen in Figure 5. This is an advantage in further developing our pPAF-AH enzyme platform, because hydrolysis of the more toxic stereoisomers of an OP will likely not be restricted.

The non-selective OP hydrolysis seen in pPAF-AH W298H may be because it has a permissive active site that allows for unrestricted binding to each of the stereoisomers of soman, as corroborated by the crystal structure of soman-adducted pPAF-AH [10]. From previous crystal structures of OP-pPAF-AH adducts with paraoxon [9] and soman [10] it became evident that binding pockets within the active site can clearly accommodate large isopropyl or pinacolyl groups with equivalent occupancy and, thereby, do not preclude specific enantiomeric preference for adduction to the active site serine. The catalytic triad of pPAF-AH (S273, H351 and D296) sits at the edge of a large trough or groove on the protein, which is possibly present to accommodate binding sites for long alkyl side chain of potentially different lengths as found in the native substrate, platelet-activating factor. The trough may be useful in assisting either substrate binding or hydrolysis product expulsion from the active site. In the BuChE G117H/E197Q mutant, a likely reason for the stereoselective hydrolysis seen may be the more restrictive nature of the active site in BuChE, which is found at the bottom of a deep gorge similar to that of AChE [18]. This active site architecture only accepts a limited number of substrates, and thus may preclude some stereoisomers from having direct access to the active site serine. We calculated the active site volume of wild-type BuChE to be 582 $Å^3$, which is similar to the volume of 496 $Å^3$ reported by other researchers [3]. Here we report the active site volume for pPAF-AH (including the trough) to be 828 $Å^3$, which is close to 1.5 times the size found in BuChE, but significantly smaller than 3,014 $Å^3$ reported for CaE [3]. The difference in active site volumes and architectural constraints, and the positioning of the catalytic triad within the active site are features that contribute to the non-stereoselective hydrolysis of soman by pPAF-AH W298H.

Variations in pH can have dramatic effects on activity. In the case of W298H, we observed enhanced activity over WT pPAF-AH across all pH levels tested, as seen in Figure 3. The shift in pH optima from WT at pH 8.0 to W298H at pH 6.9 is indicative of enhancement of an ionizable mechanism as the solution becomes more acidic. Hydrogen bonds help stabilize both intermediate and transition states within an enzyme reaction mechanism, and provide approximately 5 kcal/mole for each hydrogen bond. These stabilizing hydrogenbonds are generally localized on enzymes in defined pockets. A particular pocket known as the “oxyanion hole” present in pPAF-AH stabilizes the developing anion formed at the intermediate substrate step, with the proton donors coming directly from the amino acid residue or from the amides within the peptide backbone. For pPAF-AH, an oxyanion hole is formed by hydrogen bond interactions with the amide nitrogens of L153 and F274 [10]. BuChE has an oxyanion hole with at least three hydrogen bonding partners. Successful reactivation was achieved in BuChE when a histidine was substituted within the oxyanion hole at position 117. Potential OP hydrolase activity in the L153H pPAF-AH was anticipated because this substitution is essentially analogous to BuChE G117H. However, our L153H mutant showed no OP-hydrolase activity greater than wild-type, and was inefficient at hydrolyzing both ester substrates. We believe W298H mutant supports activation of an incoming water molecule positioned in the proper face of the phospho-

serine intermediate, analogous to BuChE G117H, without the loss of an oxyanion hole interaction, and promotes dephosphorylation to regenerate the enzyme and expel hydrolyzed nerve agent by-products.

5. CONCLUSIONS

In order to evaluate the significance of our W298H mutant, we must consider the catalytic power needed to overcome lethal concentrations of nerve agents. Recent work has demonstrated that an engineered paraoxonase-1 (PON1) needs a k_{cat} /K_M of 5×10^7 M^{-1} min^{-1} to provide protection to guinea pigs against a lethal dose of cyclosarin with no other therapeutics administered [19]. This is significantly different from the k_{cat} /K_M for our W298H at 8×10^3 M^{-1} min^{-1}. However, from a historical perspective, WT PON1 has limited catalytic power against G-type OPs [20] and yet through directed evolution, researchers have been able to optimize catalytic efficiency from <198 M^{-1} min^{-1} in WT PON1 to >1.7×10^7 M^{-1} min^{-1} in an evolved mutant [21]. Paraoxonase-1 and pPAF-AH are targeted to the same site as both are localized on HDL and LDL lipoproteins in mammalian blood. We view PAF-AH as a riskmitigating alternative platform to PON1, in the event that unanticipated problems with PON1 are discovered. PAF-AH, unlike PON1, is a serine hydrolase which has been overlooked as a platform for OP scavenger development until now. Our pPAF-AH *soman-ase* mutant (W298H) opens the door for future protein engineering projects including a directed evolution approach that is currently underway.

Acknowledgments

We thank Dr. Mark Zottola for guiding us through the Site Finder program in M.O.E. and for the many insightful discussions. Special thanks to Mr. Rick Smith and Dr. Shane Kasten for helping us on our way through the GC/MS analysis.

References

1. Taylor, P. Anticholinesterase agents. 10th. McGraw-Hill; New York: 2001.
2. Suzuki T, Morita H, Ono K, Maekawa K, Nagai R, Yazaki Y. Sarin poisoning in Tokyo subway. Lancet. 1995; 345:980. [PubMed: 7715304]
3. Maxwell, DM.; Brecht, K.; Saxena, A.; Feaster, S.; Doctor, BP. Structure and Function of Cholinesterases and Related Proteins. Plenum Press; New York: 1998. Comparison of cholinesterase and carboxylesterase as scavengers for organophosphorus compounds; p. 387-92.
4. Broomfield CA, Kirby SD. Progress on the road to new nerve agent treatments. J Appl Toxicol. 2001; 21(Suppl 1):S43–46. [PubMed: 11920919]
5. Lockridge O, Blong RM, Masson P, Froment MT, Millard CB, Broomfield CA. A single amino acid substitution, Gly117His, confers phosphotriesterase (organophosphorus acid anhydride hydrolase) activity on human butyrylcholinesterase. Biochemistry. 1997; 36:786–795. [PubMed: 9020776]
6. Millard CB, Lockridge O, Broomfield CA. Organophosphorus acid anhydride hydrolase activity in human butyrylcholinesterase: synergy results in a GDase. Biochemistry. 1998; 37:237–247. [PubMed: 9425044]
7. Geyer BC, Kannan L, Garnaud PE, Broomfield CA, Cadieux CL, Cherni I, Hodgins SM, Kasten SA, Kelley K, Kilbourne J, Oliver ZP, Otto TC, Puffenberger I, Reeves TE, Robbins N 2nd, Woods RR, Soreq H, Lenz DE, Cerasoli DM, Mor TS. Plant-derived human butyrylcholinesterase, but not an organophosphorous-compound hydrolyzing variant thereof, protects rodents against nerve agents. Proc Natl Acad Sci USA. 2010; 107:20251–20256. [PubMed: 21059932]
8. Prescott SM, Zimmerman GA, Stafforini DM, McIntyre TM. Plateletactivating factor and related lipid mediators. Annu Rev Biochem. 2000; 69:419–445. [PubMed: 10966465]

9. Montrucchio G, Alloatti G, Camussi G. Role of platelet-activating factor in cardiovascular pathophysiology. Physiol Rev. 2000; 80:1669–1699. [PubMed: 11015622]
10. Samanta U, Kirby SD, Srinivasan P, Cerasoli DM, Bahnson BJ. Crystal structures of human group-VIIA phospholipase A2 inhibited by organophosphorus nerve agents exhibit non-aged complexes. Biochem Pharmacol. 2009; 78:420–429. [PubMed: 19394314]
11. Ellman GL. Tissue sulfhydryl groups. Arch Biochem Biophys. 1959; 82:70–77. [PubMed: 13650640]
12. Kramp W, Pieroni G, Pinckard R, Hanahan D. Observations on the critical micellar concentration of 1-O-alkyl-2-acetyl-sn-glycero-3-phosphocholine and a series of its homologs and analogs. Chem Phys Lipids. 1984; 35:49–62. [PubMed: 6744496]
13. Yeung DT, Smith JR, Sweeney RE, Lenz DE, Cerasoli DM. Direct detection of stereospecific GD hydrolysis by wild-type human serum paraoxonase. FEBS J. 2007; 274:1183–1191. [PubMed: 17286579]
14. Fleming CD, Edwards CC, Kirby SD, Maxwell DM, Potter PM, Cerasoli DM, Redinbo MR. Crystal structure of human carboxylesterase 1 in covalent complexes with the chemical warfare agents soman and tabun. Biochemistry. 2007; 46:5063–71. [PubMed: 17407327]
15. Epstein TM, Samanta U, Kirby SD, Cerasoli DM, Bahnson BJ. Crystal structures of brain group-VIII phospholipase A2 in nonaged complexes with the organophosphorus nerve agents soman and sarin. Biochemistry. 2009; 48:3425–35. [PubMed: 19271773]
16. Pande AH, Tillu VA. Membrane lipid composition differentially modulates the function of human plasma platelet activating factor-acetylhydrolase. Biochim Biophys Acta. 2011; 1811:46–56. [PubMed: 20869463]
17. Benschop HP, Konings CA, Van Genderen J, De Jong LP. Isolation, anticholinesterase properties, and acute toxicity in mice of the four stereoisomers of the nerve agent GD. Toxicol Appl Pharmacol. 1984; 72:61–74. [PubMed: 6710485]
18. Nicolet Y, Lockridge O, Masson P, Fontecilla-Camps JC, Nachon F. Crystal structure of human butyrylcholinesterase and of its complexes with substrate and products. J Biol Chem. 2003; 278:41141–41147. [PubMed: 12869558]
19. Worek F, Seeger T, Goldsmith M, Ashani Y, Leader H, Sussman J, Tawfik D, Thiemann H, Wille T. Efficacy of the rePON1 mutant IIG1 to prevent cyclosarin toxicity in vivo and to detoxify structurally different nerve agents in vitro. Arch Toxicol. 2014; 88:1257–1266. [PubMed: 24477626]
20. Kirby S, Norris J, Smith J, Bahnson B, Cerasoli D. Human paraoxonase double mutants hydrolyze V and G class organophosphorus nerve agents. Chem Biol Inter. 2012; 203:181–5.
21. Gupta R, Goldsmith M, Ashani Y, Simo Y, Mullokandov G, Bar H, Ben-David M, Leader H, Margalit R, Silman I, Sussman J, Tawfik D. Directed evolution of hydrolases for prevention of G-type nerve agent intoxication. Nat Chem Biol. 2011; 7:120–5. [PubMed: 21217689]

Highlights

- Novel treatments to overcome nerve agent toxicities are being explored.
- Plasma enzymes such as serine esterases offer a unique enzymatic mechanism.
- A histidine opportunely positioned near the active site can regenerate activity.
- Mutating W298 to histidine in human pPAF-AH confers the ability to hydrolyze soman.
- Engineered enzymes which can degrade nerve agents are promising treatments.

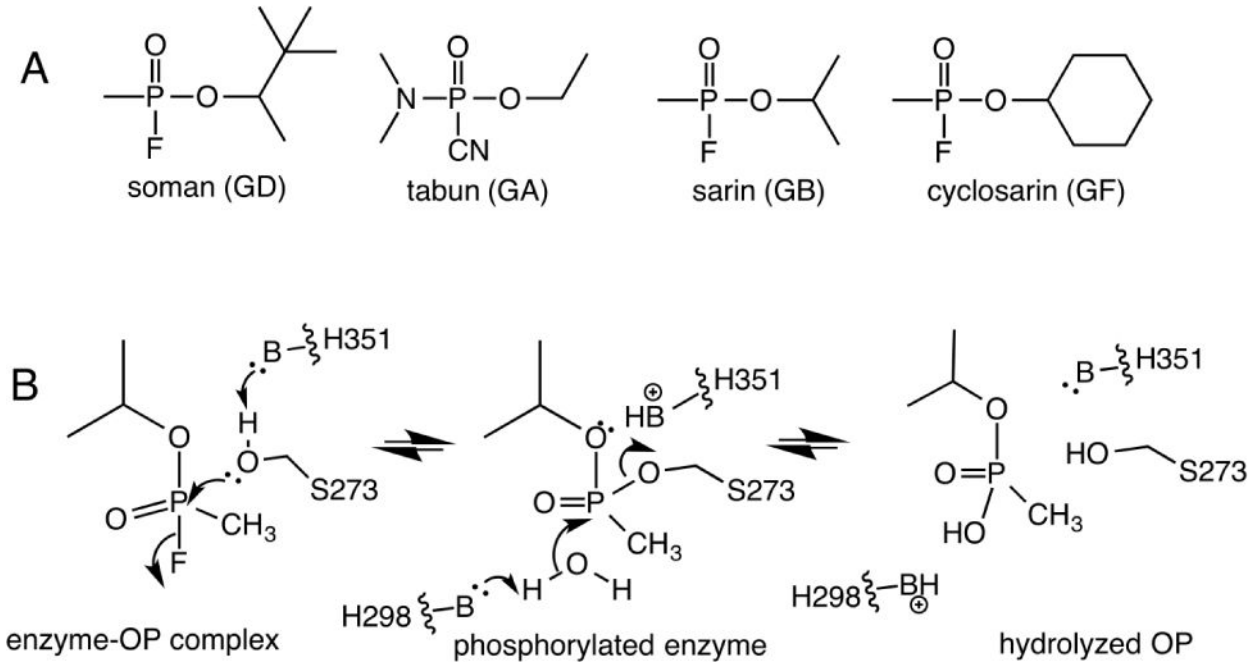

Figure 1.

Organophosphorus nerve agents react with serine hydrolases such as AChE or pPAF-AH. Panel A shows the structures of the OP compounds soman (GD), tabun (GA), sarin (GB) and cyclosarin (GF). Panel B shows the reaction of a mutant serine hydrolase with sarin as a representative OP compound. The first step forms a phosphorylated enzyme. In the second step, a water molecule is shown attacking the phosphorylated enzyme, activated by a general base catalyst (−B:; H298).

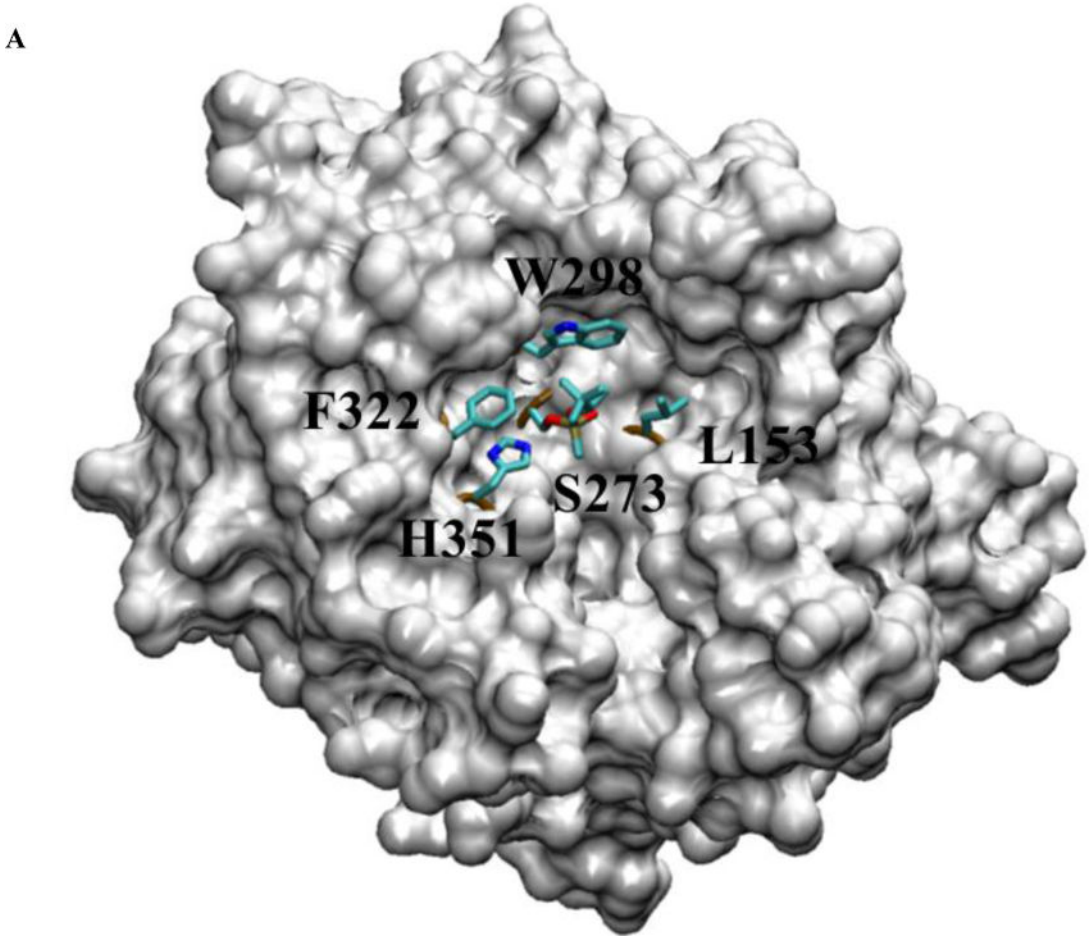

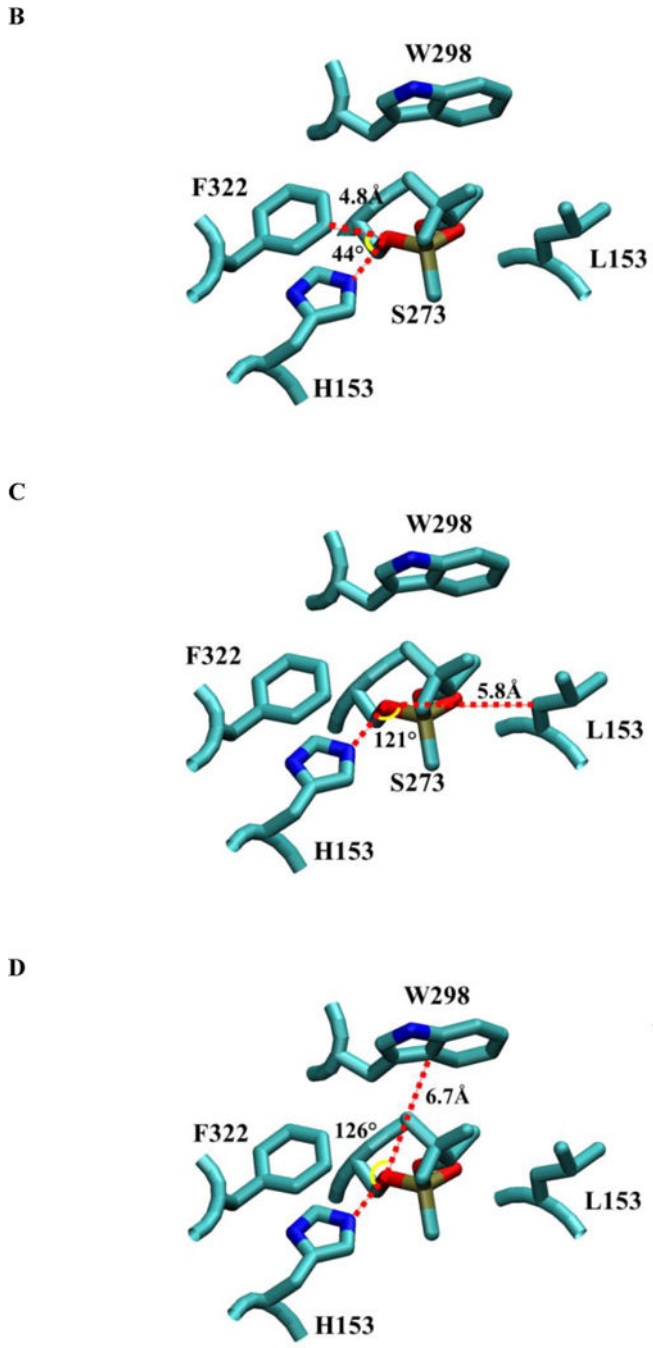

Figure 2.

The structure of pPAF-AH complexed with soman (9). Panel A shows a space-filled, partially cut-down structure of pPAF-AH with soman adducted to S273 and shows the residues surrounding the active site S273 and H351. F322, W298 and L153 are sites for mutagenesis. Panel B shows the approximate angle (yellow arc) and distance (red line) to the S273 O^{γ} for F322 if we assume S273 is the vertex and the direction to the active site histidine (H351) forms one side (red line). F322 is closest to S273 O^{γ} at 4.8 Å and sits close to H351 at approximately 44°. Panel C shows L153 is offset from H351 by approximately

121°, but it is more than 5.8 Å away from S273 Oγ. Panel D shows W298 offset from H351 by approximately 126°, and at a position of 6.7 Å from S273 Oγ.

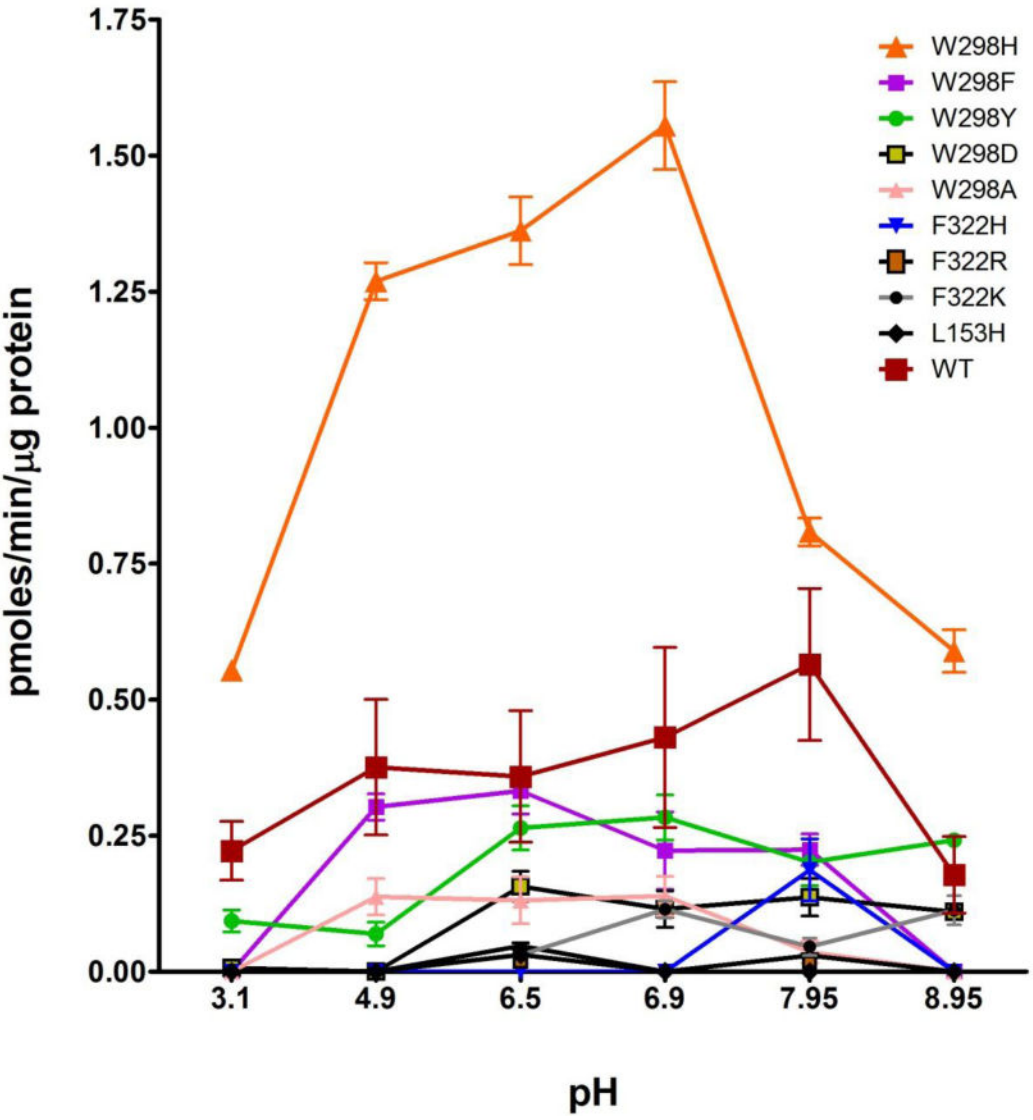

Figure 3.

Specific activity of wild-type and single point mutants of recombinant pPAF-AH at various pH levels against 2-thio PAF in 10 mM Tris buffer. Each data point is an average of three independent experiments (error bars show standard deviation).

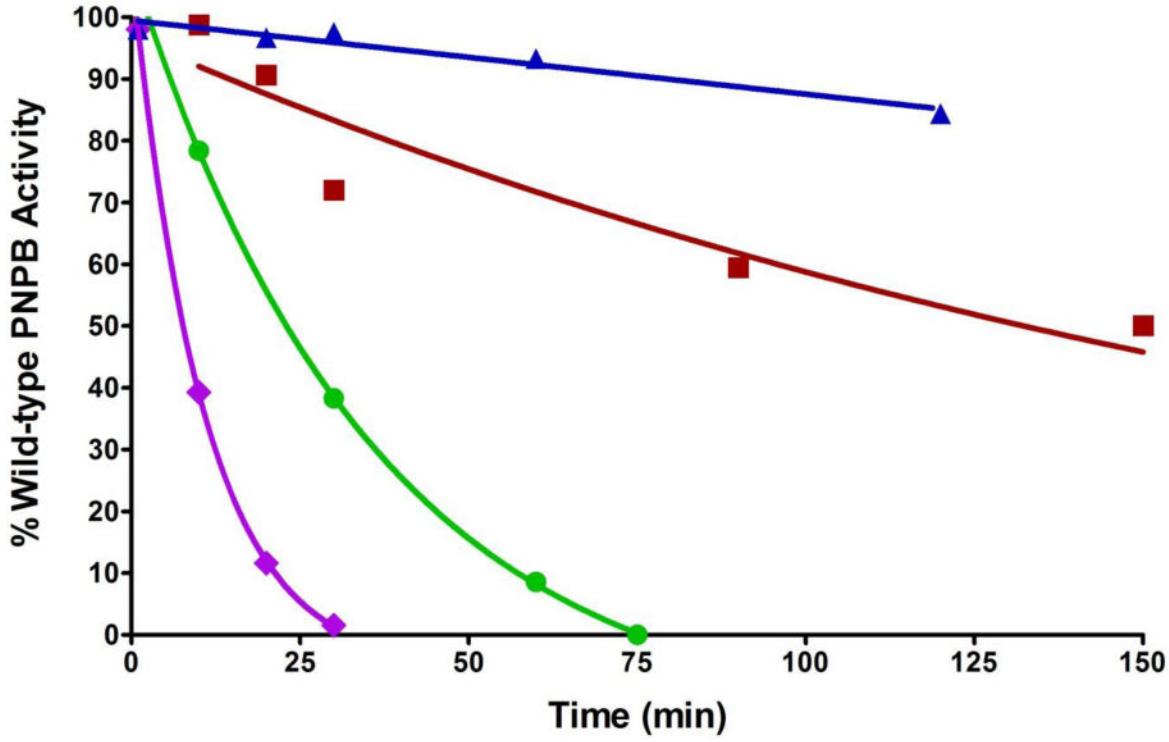

Figure 4.

A comparison of soman (GD) inhibition rates between BuChE and recombinant wild-type pPAF-AH as a function of uninhibited activity. Molar ratios of enzyme to GD are as follows: BuChE:GD 1:10 (purple diamond); pPAF-AH:GD 1:1000 (green circle); pPAF-AH:GD 1:100 (red square); pPAF-AH:GD 1:10 (blue triangle).

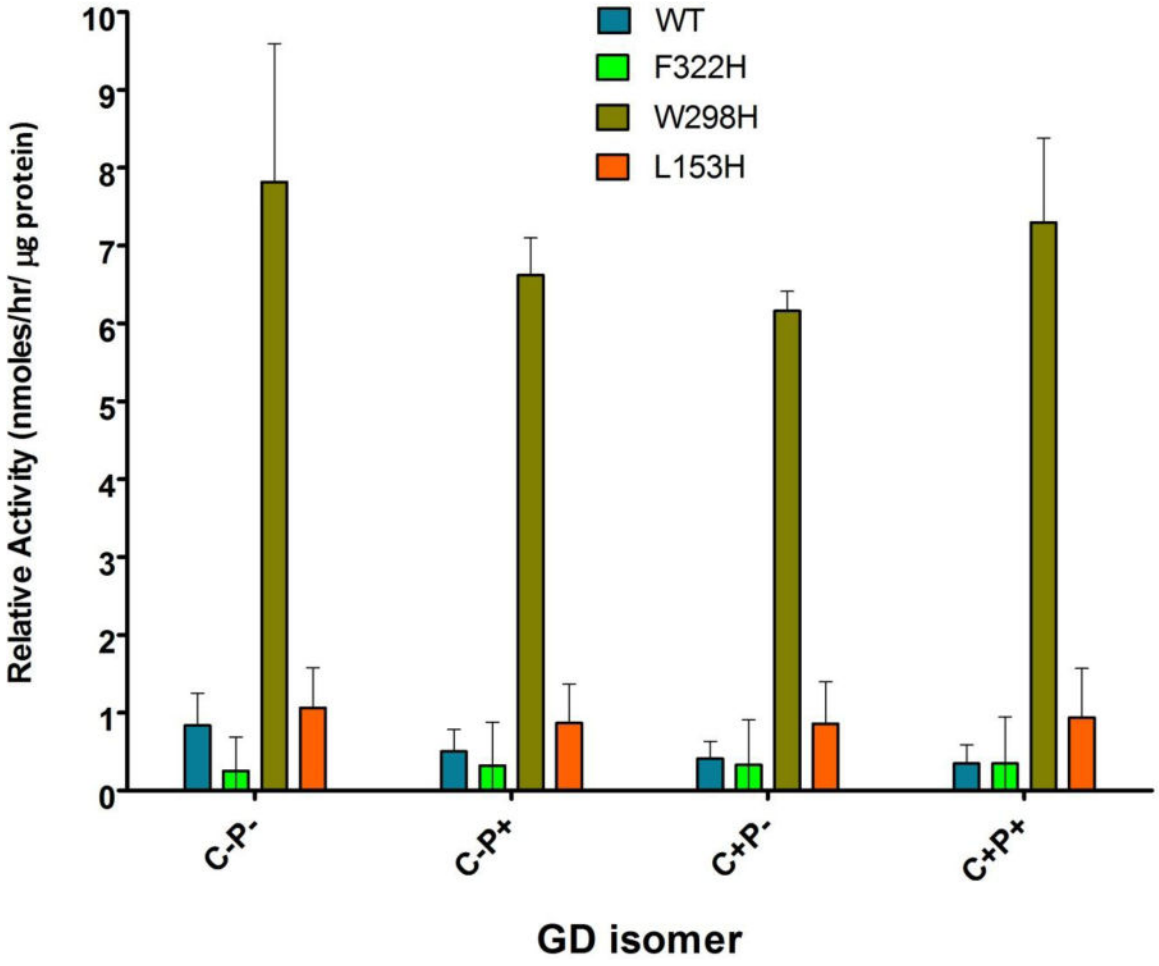

Figure 5.

Specific activity screen of histidine mutants and WT pPAF-AH for each of the four stereoisomers of soman (GD). Each bar represents the average of three independent experiments. Mock expressions were run in parallel, and their average value was subtracted from each of the experimental bars. A one-way ANOVA followed by Bonferroni's multiple comparison test determined a significant difference ($P < 0.001$) between W298H and all other mutants.

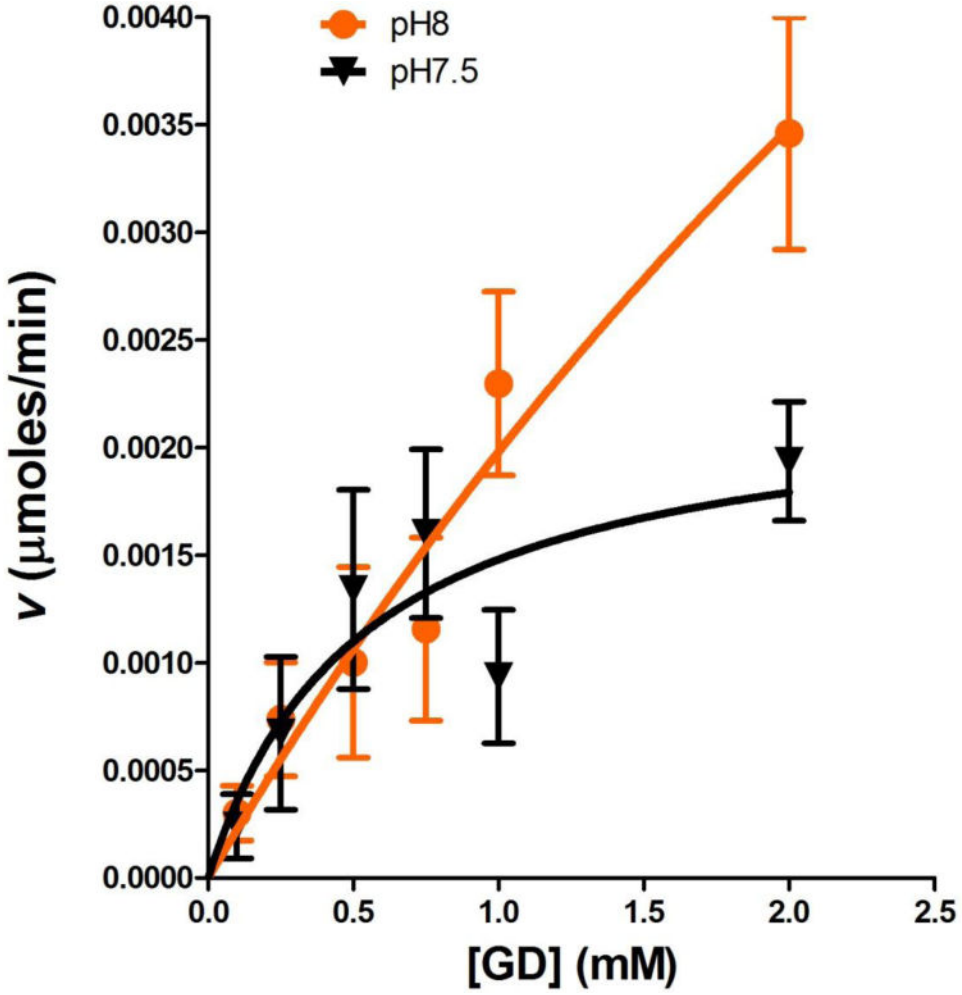

Figure 6.

Saturation kinetic curves for soman (GD) hydrolysis by W298H in 10 mM Tris buffer at pH 7.5 and pH 8.0. Rates of hydrolysis were followed across 6 substrate concentrations by GC/MS. Each point represents an average of 3 (pH 7.5) or 5 (pH 8.0) replicates ± standard deviation. Mock expression experiments were run in parallel, and subtracted from each point to account for spontaneous and nonspecific hydrolysis.

Table I

Amino Acid Residues Defining the Active Site Pocket of Plasma PAF-AH

Hydrophobic	Polar (Uncharged)	Polar (Charged)
W97, L107, F110, L111, M117, L121, L124, F125, L153, A155, F156, L159, F274, W298, F322, V350, F354, A355, F357, A360, I365, L369, L371	S108, G152, G154, Y160, S185, S273, G275, S319, Y321, Q352, N353, T358, T361	H151, H272, H351, D356, K370
56%	32%	12%

Table II

Kinetic parameters for p-nitrophenylbutyrate hydrolysis by pPAF-AH enzymes[a]

	k_{cat} (min^{-1})[b]	K_M (μM)	k_{cat}/K_M (min^{-1} μM^{-1})[b]
WT	3.5 ± 0.60	1.1 ± 0.35	3.13 ± 1.12
W298H	0.62 ± 0.07	0.66 ± 0.21	0.94 ± 0.31
W298F	0.86 ± 0.19	0.73 ± 0.42	1.18 ± 0.73
W298Y	n.d.	n.d.	n.d.
W298D	n.d.	n.d.	n.d.
W298A	n.d.	n.d.	n.d.
F322H	0.38 ± 0.08	0.53 ± 0.29	0.71 ± 0.42
F322R	0.35 ± 0.07	0.64 ± 0.35	0.54 ± 0.32
F322K	0.41 ± 0.07	0.53 ± 0.24	0.77 ± 0.36
L153H	n.d.	n.d.	n.d.

[a] The activity is reported for k_{cat} (min^{-1}) and K_M (μM) at pH 8.0 for the substrate PNPB. Each value represents an average of three independent experiments ± standard deviation. n.d. = not detected.

[b] A oneway ANOVA followed by Dunnett's test determined a significant difference ($P < 0.01$) between wildtype and all other mutants for k_{cat} and k_{cat}/K_M, but there was no significant difference in K_M.